

CHAPTER VII
GREEN HYDROCARBON PRODUCTIONS
FROM THE CATALYTIC DEHYDRATION OF BIO-ETHANOL
USING Ni, Cu, AND Pd CATALYSTS

7.1 Abstract

Metal catalysts, like Ni, Cu, and Pd, which have potential to produce hydrocarbons in various reactions such as oligomerization and polymerization, were examined in the catalytic dehydration of bio-ethanol, aiming to investigate the formation of hydrocarbons in this work, 5wt% loading of Ni, Cu, and 1 wt% loading of Pd of both metallic and metal oxide was individually loaded on an alumina support by using incipient wetness impregnation method. The catalysts were tested in the continuous U-tube reactor at 500°C for 8 hour, and later were characterized using SAA, XRD, XPS. The products were analyzed using GC-online and GC×GC-TOF/MS in order to identify the gaseous product and hydrocarbon species, respectively. As a result, it was found that metallic promoters had higher ability to produce hydrocarbons than metal oxide, resulting in the suppression in the oxygenates and hydrocarbons ratio. Moreover, the ability to produce hydrocarbons can be ranked in the order: Pd/Al₂O₃ > Ni/Al₂O₃ > Cu/Al₂O₃. For the formation of hydrocarbons, 1,3-cyclohexadiene was found as a primary hydrocarbon in the liquid products, and then converted to other hydrocarbons by various reactions. In addition, all catalysts gave similar oxygenate compounds composition; that are composed of phenols, ketones, and trace of ether compounds.

7.2 Introduction

In the last decade, hydrocarbons, such as olefins, paraffins, oligomers, and aromatics, can be produced from fossil fuel, but nowadays the attention has been changed to bio-mass as an alternative source substitute for petroleum, since crude oil price increases continuously. Additionally, there are several disadvantages of crude oil usage such as CO₂ emission, and high energy consumption, which are causes of

global warming. In Thailand, there are large quantities of bio-mass such as sugarcane, corn cobs, and cassava, which are used to produce bio-ethanol. Furthermore, bio-ethanol can be used as feedstock to produce hydrocarbons such as ethylene, propylene, oligomers, paraffins, and BTEX through catalytic dehydration reaction. Moreover, the products obtained from catalytic dehydration reaction are not only hydrocarbons but also oxygenate compounds. Generally, oxygenate compounds from ethanol can be produced via ethanol dehydrogenation reaction when a metal oxide catalyst is employed. Ethanol could undergo dehydrogenation by abstraction of hydrogen atom at anion vacancies on oxide surface, leading to aldehyde formation as primary oxygenate compound (Guan *et al.*, 2004). Furthermore, aldehyde can undergo further reaction lead to pentanone and other oxygenate compound formation. From the catalytic dehydration of bio-ethanol, oxygenate compounds are mainly composed of phenol, ketone, and ether compounds.

Moreover, metal catalysts, such as Ni, Cu, and Pd, which have potential to produce hydrocarbons are widely used in many reactions. Metallic nickel is widely used in various reactions such as hydrogenation, hydroisomerization, oligomerization and polymerization due to the low cost and high availability. Lallemand *et al.*, (2006) studied the catalytic oligomerization of ethylene over nickel-containing dealuminated Y catalysts. The catalysts were prepared by using ion-exchanged method. They found that nickel-loaded catalysts gave better activity to produce oligomers as the desired product at a reaction temperature of 50°C, and 35 MPa ethylene pressure. The products consisted of C₄-C₁₂ unsaturated aliphatic hydrocarbons, especially C₄ as the dominant product. Moreover, heterogeneous nickel-supported HBETA catalysts for ethylene oligomerization was proposed by Martinez *et al.*, (2013). Their results showed that Ni²⁺ species were responsible to the initiation of ethylene and the undertaking oligomerization. Moreover, they found that the amount of nickel loading responsible for the product distribution. Nickel-supported Al₂O₃ catalysts in propene oligomerization were studied by Cai (1990). Their results showed that the hydrocarbons obtained were in the range of C₆ to C₁₈ hydrocarbons. In 2004, nickel-supported MCM41 catalysts for ethylene oligomerization was studied by Hulea *et al.*, (2004). Their results showed that the hydrocarbon products were in the range of C₆ to C₁₄ hydrocarbons, and C₆ products were methyl-pentane, 1-hexene, and its isomers.

Additionally, copper bromide over TiO_2 substrate was examined in ATRP polymerization for producing polystyrene by Barthelemy *et al.*, 2011. They found that copper bromide can initiate styrene polymerization, and the obtained product was high molecular weight polystyrene. A CuCl catalyst for styrene polymerization was studied by Cheng *et al.*, 2005. The results showed that CuCl can encourage styrene polymerization, and the product was polystyrene in linear form. In addition, metal catalysts can be divided into two main groups; that are noble and non-noble metal catalyst. Generally, Ni and Cu are widely used as catalysts in various reactions, aiming to produce hydrocarbons. Moreover, noble metal catalysts, like Pd, are widely used in various reactions as well because it has high catalytic activity to stimulate the reactions. Li *et al.*, 2002 studied a synthesized palladium complex catalyst for ethylene polymerization. Their results showed that the catalyst exhibited high catalytic activity, and the obtained product was HDPE. (Pyrazolo-1-yl) carbonyl palladium complex catalyst for ethylene polymerization was studied by Mkoyi *et al.*, 2013. They revealed that the catalyst exhibited moderate catalytic activity, and the obtained product was linear HDPE. Additionally, palladium catalysts also have potential to promote cross-couplings, hydrogenation, and isomerization (Musolino *et al.*, 2010)

Therefore, noble metal (Pd) and non-noble (Ni and Cu) metal-promoted in both metal and metal oxide forms are an interesting catalyst in the catalytic dehydration of bio-ethanol because they have high ability to produce hydrocarbons. Therefore, the aim of this work was to investigate the effects of metals and their oxidation state in product distribution. The ability on transformation of ethanol to oxygenates and hydrocarbons was compared. Furthermore, the catalysts were characterized using surface area analyzer (SAA), X-ray diffraction spectroscopy (XRD), and X-ray photoelectron spectroscopy (XPS).

7.3 Experimental

7.3.1 Catalyst Preparation

$\gamma\text{-Al}_2\text{O}_3$ (γ -Alumina) used in this work was supplied from Sigma Aldrich, Singapore. Nickel (II) nitrate hexahydrate, copper (II) nitrate nonahydrate,

and palladium (II) hydrate were used as nickel, copper, and palladium precursors. A metal solution was loaded on the support using incipient wetness impregnation technique until the amounts of 5.0 wt% Ni, Cu loading, and 1 wt% Pd were achieved. After impregnation, the wet catalysts were dried at 110°C overnight, and then calcined, starting from room temperature with the heating rate of 10°C/min to 600°C then held for 3 hours. After that the calcined catalysts were pelletized, crushed, and sieved to 20-40 mesh particles. Additionally, to produce the reduced catalysts, the calcined catalysts were pretreated under H₂ atmosphere follow below conditions.

Table 7.1 Catalyst pretreatment conditions.

Sample	Temperature (°C)		Time Interval (hr)
	Start	Final	
Ni/Al ₂ O ₃	30	550	2
Cu/Al ₂ O ₃	30	550	2
Pd/Al ₂ O ₃	30	400	2

7.3.2 Catalytic Dehydration of Bio-ethanol

The catalytic dehydration of bio-ethanol was performed in a continuous isothermal fixed-bed U-tube reactor controlled at 500°C under atmospheric pressure for 8 hours. The high purity grade bio-ethanol (99.5%) was fed by a syringe pump with carrier gas, helium, through the catalyst bed. The gaseous product was passed through an online-GC, and the liquid condensed in a cooling unit was collected, and after 8 hour time-on-stream, the oil was extracted from the liquid product by using carbon disulfide.

7.3.3 Product Analysis

The gaseous products were analyzed by using a GC-TCD (Agilent 6890N) to determine the gas composition, and GC-FID (Agilent 6890N) was used to determine the bio-ethanol and oxygenate contents. The extracted oils were analyzed by using Gas Chromatography (Agilent technology 7890) with Time-of-Fight Mass Spectrometer (LECO, Pegasus® 4D TOF/MS) equipped with the 1st GC column was

a non-polar Rtx®-5sil MS (30 m × 0.25 mm × 0.25 μm), and the 2nd GC column was an Rxi®-17 MS column (1.790 m × 0.1 mm ID × 0.1 μm) to determine the composition.

7.3.4 Catalyst Characterization

The Brunauer-Emmett-Teller (BET) technique was used to determine the specific surface area, total pore volume, and pore size of catalysts using Thermo Finnigan/Sorptomatic 1990 surface area analyzer. The pore size distribution was calculated using BJH method. The X-ray diffraction of catalysts was determined using RigaguSmartLab® in BB/Dtex mode with CuKα radiation. The machine collected the data from 10°-80° (2θ) at 5°/min with the increment of 0.01°. X-ray Photoelectron Spectroscopy (XPS) spectra were carried out using a AXIS ULTRA^{DLD}. The system was equipped with a monochromatic Al x-ray source and hemispherical analyzer. The spectrometer was operated with the pass energy of 160 and 40 eV for wide and narrow scan, respectively. All peaks were calibrated from referring C 1s spectra located at 284.8eV

7.4 Catalyst Characterization

7.4.1 XRD

The XRD pattern and 2-theta values of commercial γ-alumina, and Ni-, Cu-, and Pd-modified Al₂O₃ in both metallic and metal oxide forms are shown in Figure 7.2 and Table 7.2. The characteristic peak of γ-alumina can be detected at 2θ = 67.5° (Liu *et al.*, 2012) from all catalysts. Moreover, the peak of NiO is detected at 2θ = 43.9 (Li *et al.*, 2006) whereas the peak of metallic nickel is detected at 2θ = 44.5°, which represents the fcc of metallic nickel (Li *et al.*, 2006). For the XRD patterns of copper oxide and metallic Cu on alumina surface, the diffraction peak due to Cu₂O is detected at 2θ = 42.7° (Guo *et al.*, 2009), and the diffraction peak due to metallic Cu is detected at 2θ = 43.8 (Guo *et al.*, 2009). Furthermore, the XRD patterns of calcined and reduced catalysts are shown in Figure 7.1. It can be noticed the peak due to metallic Pd is detected at 2θ = 42.4° (Huang *et al.*, 2006). The peaks due to PdO is detected at 2θ = 33.6°, and 40.2° (Huang *et al.*, 2006). As a result, the

metal oxide of Ni, Cu, and Pd is formed on the surface of alumina, and the metallic Ni, Cu, and Pd is present on the surface of the reduced catalyst. Therefore, the preparation of NiO/Al₂O₃, Cu₂O/Al₂O₃, PdO/Al₂O₃, Ni/Al₂O₃, Cu/Al₂O₃, and Pd/Al₂O₃ were proven successful.

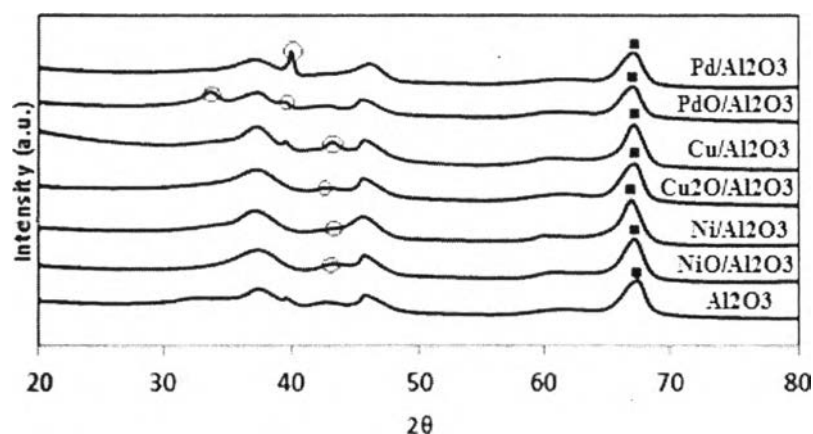


Figure 7.1 XRD patterns of commercial γ -Al₂O₃, Ni-, Cu-, and Pd-modified Al₂O₃.

Table 7.2 2-theta of each elements on alumina surface

Element	2θ	
	Metallic	Metal Oxide
Ni	44.5	43.9
Cu	43.8	40.7
Pd	42.4	33.6, 40.2

7.4.2 Surface Composition

To further verify the chemical state of nickel, copper, and palladium on the surface of samples. X-ray Photoelectron Spectroscopy was employed, and the results are shown in Figure 7.2. Figure 7.2 (a) displays the XPS spectrum Ni/Al₂O₃ catalyst. The Ni 2p_{3/2} binding energies located at 852.2, 855.2, and 858.3 eV are assigned to Ni(0), NiO (Biesinger *et al.*, 2011), and NiAl₂O₄ (Salagre *et al.*, 1996), respectively; which account for 62.9% Ni, 7.5% NiO, and 29.6% NiAl₂O₄ as depicted in Figure 7.3 (a). Moreover, the characteristic satellite peak of Ni²⁺ is

observed at 861.4 eV (Salagre *et al.*, 1996). For spent Ni/Al₂O₃ catalyst, Figure 7.2 (a2) exhibits that the Ni 2p_{3/2} binding energies at 852.0, 855.8 and 858.7 eV are assigned to Ni⁽⁰⁾, NiO (Biesinger *et al.*, 2011), and NiAl₂O₄ (Salagre *et al.*, 1996); which are accounted for 6.1% Ni, 77.5% NiO, and 16.4% NiAl₂O₄, respectively. Additionally, the characteristic satellite peak of Ni²⁺ is also observed at 862.3 eV (Salagre *et al.*, 1996). In addition, the XPS spectra of both fresh and spent NiO/Al₂O₃ catalysts are illustrated in Figure 7.2 (a3) and (a4), respectively. Figure 7.2 (a3) shows that the Ni 2p_{3/2} binding energies at 855.6 eV is assigned to NiO (Biesinger *et al.*, 2011), accounted for 100% NiO. Additionally, the peak at 861.6 eV is assigned to the characteristic satellite peak of Ni²⁺ (Salagre *et al.*, 1996). For the spent NiO/Al₂O₃ catalyst illustrated in Figure 7.2 (a4), the Ni 2p_{3/2} binding energies at 855.2 and 857.5 eV are assigned to NiO and Ni(OH)₂ (Biesinger *et al.*, 2011). Furthermore, the peak at 861.4 eV is assigned to the characteristic peaks of peak Ni²⁺ (Salagre *et al.*, 1996). From the results, fresh Ni/Al₂O₃ catalyst consists of 62.9% Ni, 7.5% NiO, and 29.6% NiAl₂O₄. However, fresh NiO/Al₂O₃ catalyst consists of 100% NiO. After the catalytic testing, Ni/Al₂O₃ catalyst is reduced; so, the surface is composed of 6.1% Ni, 77.5% NiO and 16.4% NiAl₂O₄. In addition, the surface of spent NiO/Al₂O₃ is composed of 89.5% NiO and 10.5% Ni(OH)₂.

Figure 7.2 (b1) displays the XPS spectrum of Cu/Al₂O₃ catalyst. The Cu 2p_{3/2} binding energies located at 932.6 and 934.8 eV are assigned to Cu⁽⁰⁾ (Biesinger *et al.*, 2010) and CuO (Hodgkinson *et al.*, 2013), accounted for 92.8% and 7.2%, respectively. Moreover, the characteristic satellite of Cu²⁺ is observed at 942.9 eV (Akgul *et al.*, 2014). For spent Cu/Al₂O₃ catalyst, Figure 7.2 (b2) exhibits that the Cu 2p_{3/2} binding energies at 932.0 and 943.6 eV are assigned to Cu₂O and CuO (Hodgkinson *et al.*, 2013), accounted for 77.4% and 22.6%, respectively. Additionally, the two-overlapped characteristic satellite peaks of Cu²⁺ are also observed at 940.9 and 943.6 eV (Akgul *et al.*, 2014). In addition, the XPS spectra of both fresh and spent Cu₂O catalysts are illustrated in Figure 7.2 (b3) and (b4), respectively. Figure 7.2 (b3) shows that the Cu 2p_{3/2} binding energies at 932.5 and 934.7 eV are assigned to Cu₂O (Biesinger *et al.*, 2010) and CuO (Biesinger *et al.*, 2010); accounting for 79.1% and 20.9%, respectively. Additionally, the peaks at 941.6 and 943.5 eV are assigned to the characteristic satellite peaks of Cu²⁺

(Akgul *et al.*, 2014). For the spent $\text{Cu}_2\text{O}/\text{Al}_2\text{O}_3$ catalyst illustrated in Figure 7.2 (b4), the Cu $2p_{3/2}$ binding energies at 932.6 and 935.4 eV are assigned to Cu_2O and CuO (Akgul *et al.*, 2014), accounted for 75.5% and 24.5%, respectively. Furthermore, the peak at 786.9 eV is assigned to the characteristic peaks of Cu^{2+} (Akgul *et al.*, 2014). From the results, the surface of fresh $\text{Cu}/\text{Al}_2\text{O}_3$ catalyst consists of 92.8% Cu and 7.2% CuO . Moreover, the surface of $\text{Cu}_2\text{O}/\text{Al}_2\text{O}_3$ catalyst consists of 79.1% Cu_2O and 20.9% CuO . After the catalytic testing, $\text{Cu}/\text{Al}_2\text{O}_3$ catalyst is oxidized; so, the surface is composed of 77.4% Cu_2O and 22.6% CuO , as displayed in Figure 7.3(b). In addition, the surface of spent $\text{Cu}_2\text{O}/\text{Al}_2\text{O}_3$ catalyst is composed of 75.5% Cu_2O and 24.5% CuO , indicating that Cu_2O is a stable phase in the catalytic dehydration of bio-ethanol.

Figure 7.2 (c1) displays the XPS spectrum $\text{Pd}/\text{Al}_2\text{O}_3$ catalyst. The Pd $3d_{5/2}$ binding energy located at 335.1 is assigned to $\text{Pd}^{(0)}$ (Brun *et al.*, 1999), accounting for 100% Pd on Al_2O_3 surface. For spent $\text{Pd}/\text{Al}_2\text{O}_3$ catalyst, Figure 7.2 (c2) exhibits that the Pd $3d_{5/2}$ binding energies at 335.1 and 336.9 eV are assigned to $\text{Pd}^{(0)}$ and PdO (Brun *et al.*, 1999); accounting for 82.7% Pd and 14.3% PdO , respectively. In addition, the XPS spectra of both fresh and spent $\text{PdO}/\text{Al}_2\text{O}_3$ catalysts are illustrated in Figure 7.2 (c3) and (c4), respectively. Figure 7.2 (c3) shows that the Pd $2d_{5/2}$ binding energy at 336.6 eV is assigned to PdO (Brun *et al.*, 1999), accounted for 100% PdO on Al_2O_3 surface, respectively. For the spent $\text{PdO}/\text{Al}_2\text{O}_3$ catalyst illustrated in Figure 7.2 (c4), the Pd $3d_{5/2}$ binding energies at 335.6 and 337.7 are assigned to metallic Pd and PdO (Brun *et al.*, 1999); accounting for 96.6% Pd and 3.4% PdO , respectively. From the results, the surface of fresh $\text{Pd}/\text{Al}_2\text{O}_3$ catalyst consists of 100% Pd, as shown in Figure 7.3(c). Moreover, the surface of $\text{PdO}/\text{Al}_2\text{O}_3$ consists of 100% PdO . After the catalytic testing, $\text{Pd}/\text{Al}_2\text{O}_3$ catalyst is partially reduced; so, the surface is composed of 82.7% Pd and 17.3% PdO . On the other hand, the surface of spent $\text{PdO}/\text{Al}_2\text{O}_3$ is composed of 96.6% Pd and 3.4% PdO because the reduction of PdO takes place during the reaction.

Table 7.3 Binding energies (eV) of Ni-, Cu-, and Pd-modified catalysts

Sample		Main Peaks		Sat. Shake Up		% Composition	
		Fresh	Spent	Fresh	Spent	Fresh	Spent
Ni/Al ₂ O ₃	Ni	852.2	582			62.9	6.1
	NiO	855.2	855.8	861.4	862.3	7.5	77.5
	NiAl ₂ O ₃	858.3	858.7			29.6	16.4
NiO/Al ₂ O ₃	NiO	855.2	855.2	861.4	861.4	100	89.5
	Ni(OH) ₂	-	857.5				10.5
Cu/Al ₂ O ₃	Cu	932.6	-		940.9	92.8	-
	Cu ₂ O	-	932	942.9	943.6	-	77.4
	CuO	934.8	934.6			7.2	22.6
Cu ₂ O/Al ₂ O ₃	Cu ₂ O	932.5	932.6	941.6	942.1	79.1	75.5
	CuO	934.7	934.7	943.5		20.9	24.5
Pd/Al ₂ O ₃	Pd	335.1	335.1			100	82.7
	PdO	-	336.9	-	-	-	17.3
PdO/Al ₂ O ₃	Pd	-	335.6			-	96.6
	PdO	336.6	337.7			100	3.4

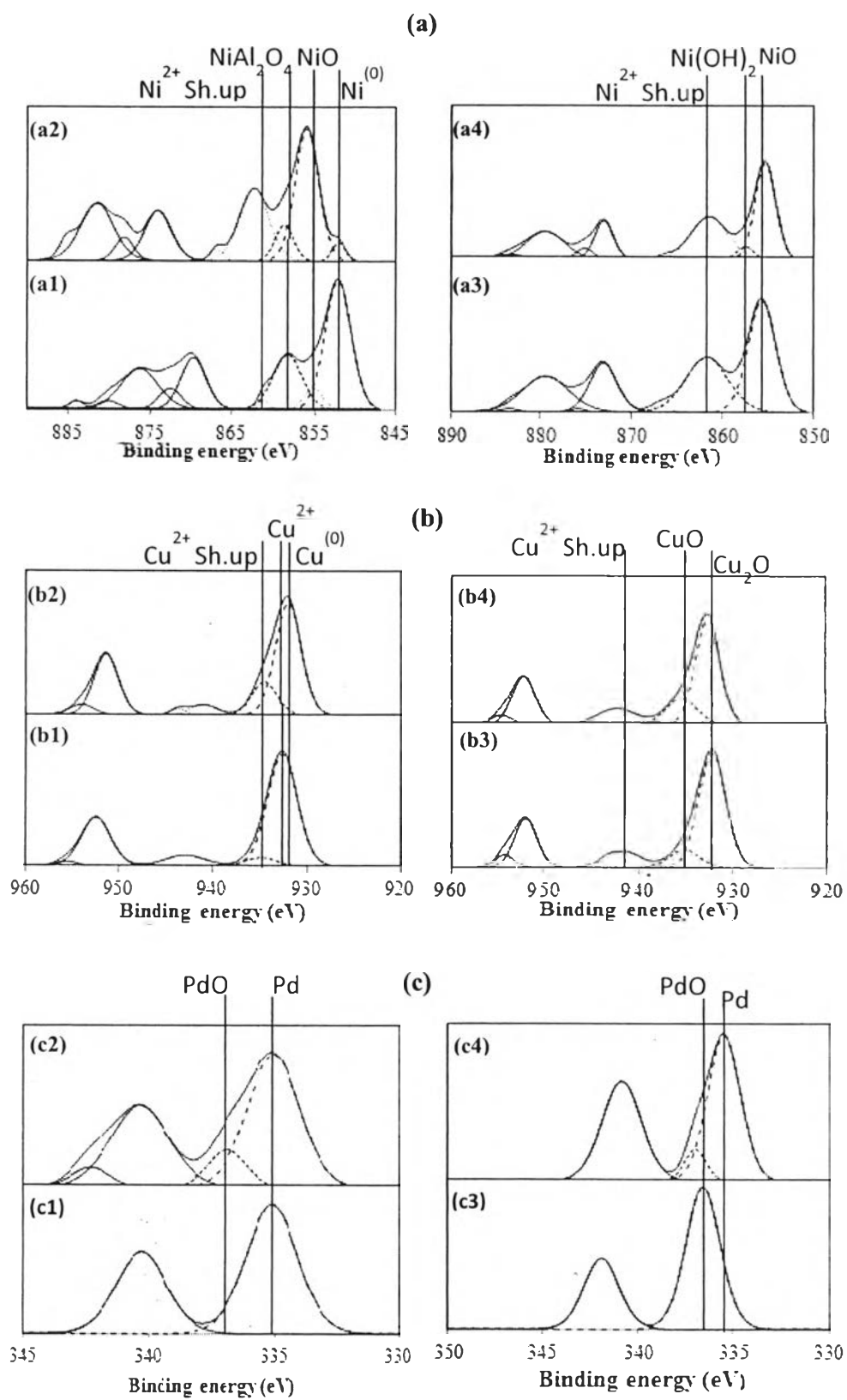


Figure 7.2 XPS spectra of (a) Ni-, (b) Cu-, and (c) Pd-modified catalysts.

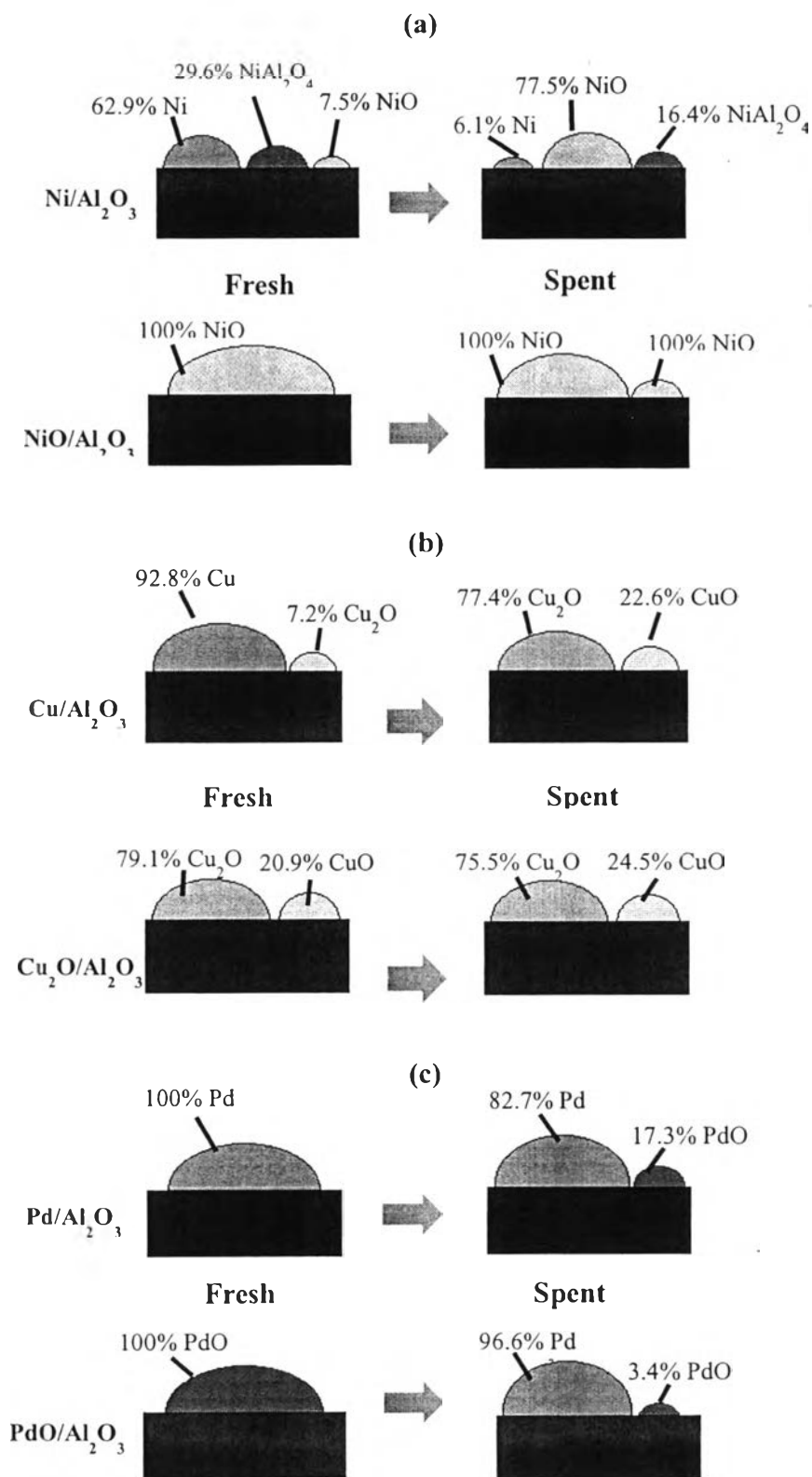


Figure 7.3 Surface compositions of Ni-, Cu-, and Pd-modified catalysts.

7.4.3 Physical Properties

Table 7.4 Physical properties of un-modified and modified catalysts

Sample	Surface Area (m ² /g) ^a	Pore Volume (cm ³ /g) ^a	Pore Diameter (nm) ^b
Al ₂ O ₃	148.6	0.55	45.32
NiO/Al ₂ O ₃	139.7	0.43	44.67
Ni/Al ₂ O ₃	127.4	0.35	33.28
Cu/Al ₂ O ₃	140.7	0.42	39.67
Cu ₂ O/Al ₂ O ₃	129.5	0.37	37.52
PdO/Al ₂ O ₃	142.8	0.63	39.43
Pd/Al ₂ O ₃	136.5	0.38	52.39

^a determined using BET method

^b determined using B.J.H method

Table 7.4 shows the specific surface area, pore volume, and pore diameter of unmodified γ -alumina and modified alumina determined using Barrett-Joyner-Halunda (BJH) method. As shown in Table 7.4. it is observed that surface area and pore volume decrease when metallic and metal oxide forms of Ni, Cu, and Pd was individually loaded on the alumina surface due to the solution of metal precursor adsorbed deeply in the pore, resulting in the formation of metallic and metal oxide inside the pore.

7.5 Product Yields and Gas Composition

7.5.1 Product Yields

Table 7.5 Product yields obtained from using Ni-, Cu-, and Pd-modified catalysts

Sample	% Yield			Conversion
	Oil	Water	Gas	
Al ₂ O ₃	3.1	20.6	76.3	98.7
Ni/Al ₂ O ₃	3.9	8.4	87.8	99.3
NiO/Al ₂ O ₃	3.2	13.4	83.5	98.9
Cu/Al ₂ O ₃	5.3	25.3	69.4	97.7
Cu ₂ O/Al ₂ O ₃	4.7	15.7	79.7	98.4
Pd/Al ₂ O ₃	1.9	4.5	93.6	99.3
PdO/Al ₂ O ₃	2.8	2.8	94.4	97.6

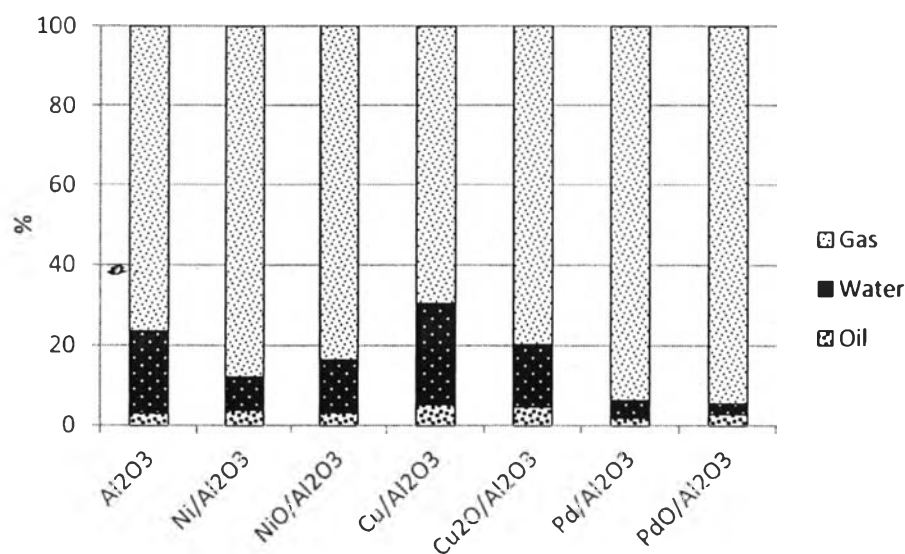


Figure 7.4 Product yields obtained from using Ni-,Cu-, and Pd-modified catalysts.

From the catalytic testing, ethanol conversion in Table 7.5 shows that the conversions are significantly different for all catalysts. This means that ethanol can convert to ethylene easily at the reaction temperature. In addition, the product

yields obtained from all catalysts are shown in Table 7.5 and Figure 7.4. It is noticed that all catalysts give mostly gaseous products with a small amount of oil yield. Moreover, the yield of water is suppressed in almost all samples, except for Cu/Al₂O₃ catalysts.

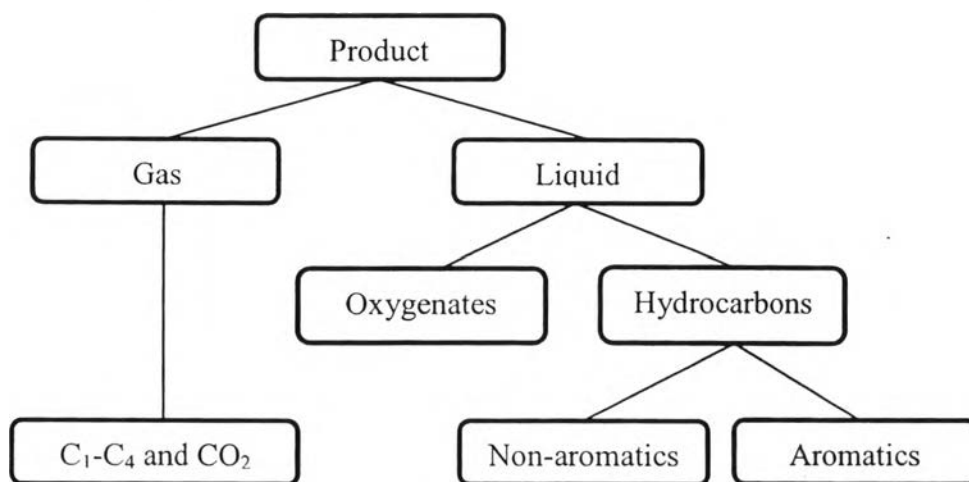


Figure 7.5 Possible products obtained from the catalytic dehydration of bio-ethanol.

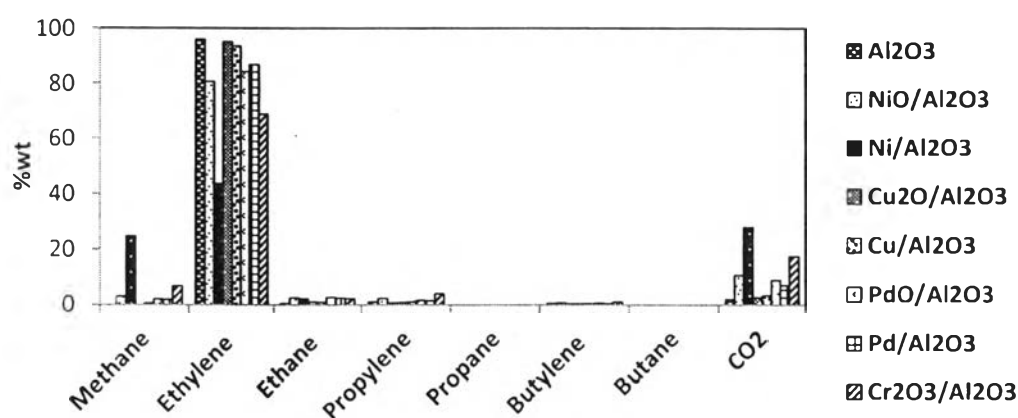
7.5.2 Gas Composition

Figure 7.6 and Table 7.6 present gaseous product composition obtained from using Ni-, Cu-, and Pd-modified catalyst. As a result, it is observed that ethylene is made considerably from all catalysts. Furthermore, ethylene is significantly suppressed from 96.0 wt% to 43.8 wt%.; on the other hand, methane is significantly enhanced from 0.00 wt% to 24.9 wt% using Ni/Al₂O₃ catalyst. This indicates that metallic Ni favors to promote ethylene cracking in ethanol dehydration. Moreover, the other gaseous product, for examples, ethane, propylene, and butylene, are slightly enhanced. Additionally, when using other catalysts, like Cu- and Pd-modified catalysts in both metallic and metal oxide forms, ethylene is also found as the major component, and the other gaseous products are present in a trace amount as shown in Figure 7.6 and Table 7.6, respectively.

Table 7.6 Gas product composition obtained from bio-ethanol dehydration

Sample	Concentration (wt%)							
	CH ₄	C ₂ H ₂	C ₂ H ₄	C ₃ H ₆	C ₃ H ₈	C ₄ H ₈	C ₄ H ₁₀	CO ₂
Al ₂ O ₃	0.0	96.0	0.5	1.0	0.0	0.5	0.0	2.1
Ni/Al ₂ O ₃	24.9	43.8	2.2	0.7	0.0	0.3	0.0	28.1
NiO/Al ₂ O ₃	3.1	80.6	2.6	2.3	0.0	0.7	0.0	10.7
Cu/Al ₂ O ₃	0.6	93.5	0.9	1.1	0.0	0.4	0.0	3.4
Cu ₂ O/Al ₂ O ₃	0.0	95.1	1.0	0.9	0.0	0.3	0.0	2.7
Pd/Al ₂ O ₃	1.9	86.7	2.5	1.5	0.0	0.4	0.0	7.0
PdO/Al ₂ O ₃	2.1	84.2	2.7	1.6	0.0	0.6	0.0	8.9

Data were taken at the eight hour of time-on-stream

**Figure 7.6** Gas product composition obtained from bio-ethanol dehydration.

7.6 Liquid Products

7.6.1 Liquid Product Distribution

The liquid product distribution in Figure 7.7 and Table 7.7 shows that the liquid product composes of oxygenate compounds and hydrocarbons. Compared to unmodified Al₂O₃, all promoted-catalysts in both metallic and metal oxide forms suppress the formation of oxygenate compounds with increasing hydrocarbon formation. Moreover, the hydrocarbon formation is enhanced from 7.9 wt% to 16.1 wt%, 12.8 wt%, and 60.4 wt% using Ni/Al₂O₃, Cu/Al₂O₃, and Pd/Al₂O₃ catalyst,

respectively. In addition, the hydrocarbons are also enhanced from 7.9 wt% to 10.2, 11.3, and 24.5 wt% using NiO/Al₂O₃, Cu₂O/Al₂O₃, and PdO/Al₂O₃ catalyst, respectively. The results indicate that the catalysts in metallic forms can promote higher hydrocarbon production than metal oxide forms, and among the metal catalysts, Pd/Al₂O₃ gives the highest hydrocarbon production due to more surface stability and less surface sensitivity. Furthermore, the hydrocarbon production can be ranked in the order: Pd/Al₂O₃ > Ni/Al₂O₃ > Cu/Al₂O₃ > Al₂O₃.

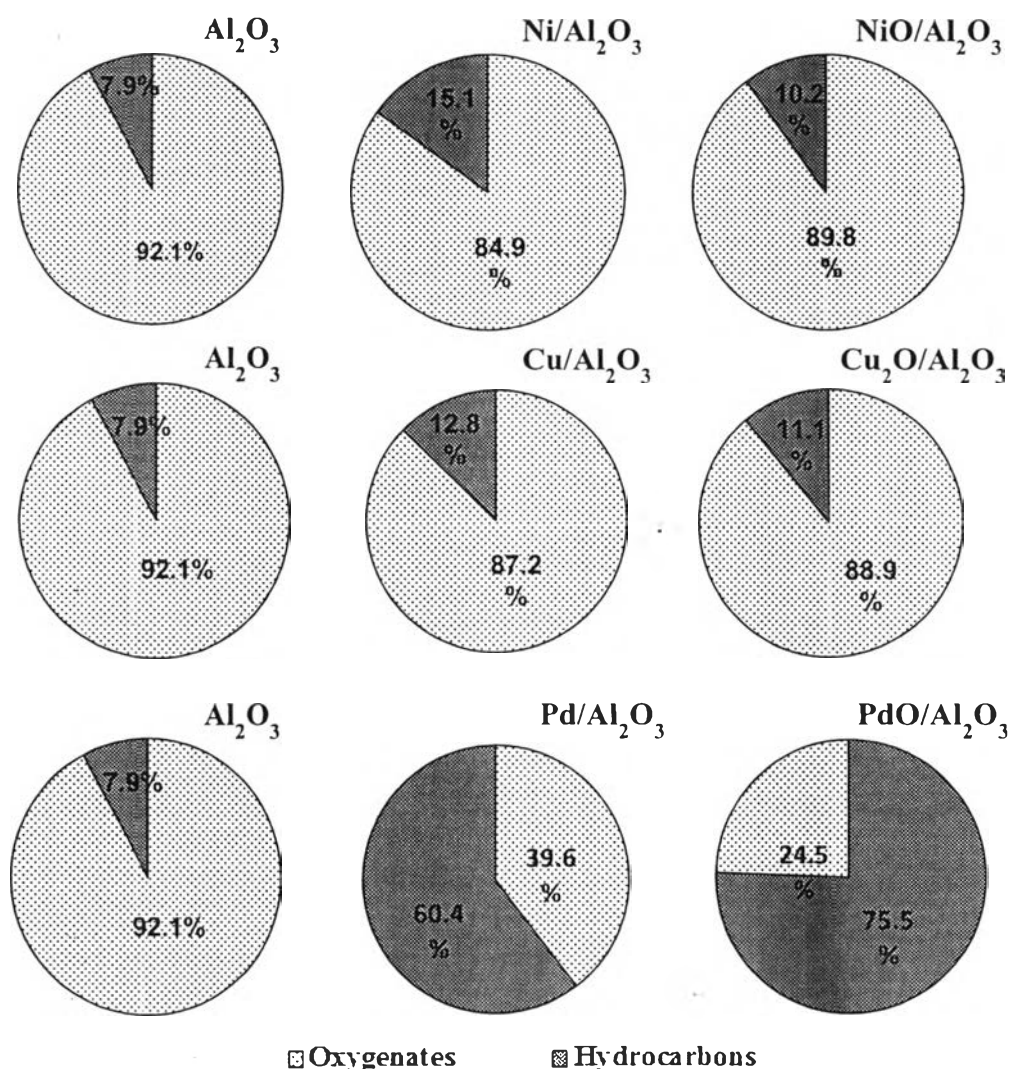


Figure 7.7 Liquid product distribution obtained from using Ni-, Cu-, and Pd-modified catalysts.

Table 7.7 Liquid product distribution obtained from bio-ethanol dehydration

Sample	Distribution (wt%)	
	Oxygenates	Hydrocarbons
Al ₂ O ₃	92.1	7.9
Ni/Al ₂ O ₃	84.9	15.1
NiO/Al ₂ O ₃	89.8	10.2
Cu/Al ₂ O ₃	87.2	12.8
Cu ₂ O/Al ₂ O ₃	88.9	11.1
Pd/Al ₂ O ₃	39.6	60.4
PdO/Al ₂ O ₃	75.5	24.5

7.6.2 Hydrocarbon Compositions

Figure 7.8 presents hydrocarbon compositions obtained from using Ni-, Cu-, and Pd-modified Al₂O₃ catalysts in both metallic and metal oxide forms. As a result, hydrocarbons are composed of non-aromatics, benzene, toluene, mixed-xylenes, C₉-, and C₁₀+aromatics. Furthermore, most of the hydrocarbons distribute in C₆ product; that is, benzene. Among these catalysts, Pd/Al₂O₃ shows the significant increase in C₁₀+aromatics because Pd on Al₂O₃ has high hydrocarbon production and large pore size of alumina support. From Tables 7.8, 7.9, and 7.10, it can be noticed that, using Ni-, Cu-, and Pd-modified Al₂O₃ catalyst in both metallic and metal oxide forms, there is non-aromatics formation. In non-aromatics, 1,3-cyclohexadiene is found as a main component from all catalysts.

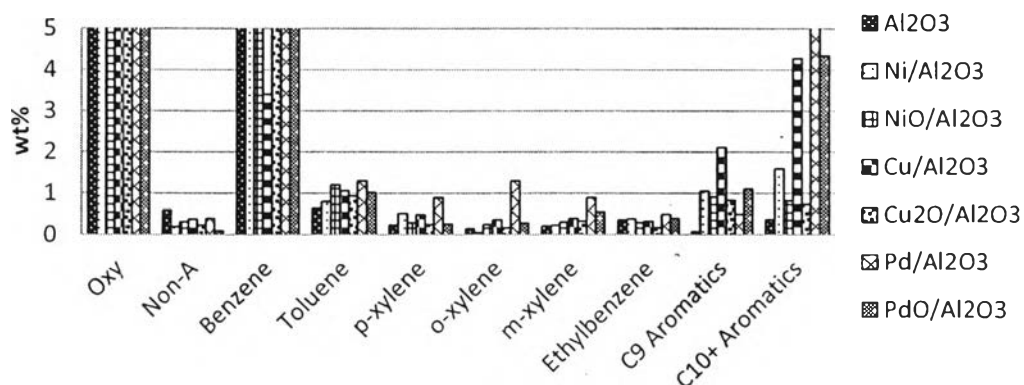
**Figure 7.8** Compositions of hydrocarbons obtained from using Ni-, Cu-, and Pd-modified catalysts.

Table 7.8 Composition of hydrocarbons obtained from using Ni-modified catalysts

Product	Sample		
	A ₂ O ₃	Ni/Al ₂ O ₃	NiO/Al ₂ O ₃
Product Distribution (wt%)			
Oxygenatess	92.1	84.9	89.8
Non-aromatics	0.60	0.20	0.30
Benzene	5.20	10.2	5.70
Toluene	0.60	0.80	1.20
p-Xylene	0.20	0.50	0.30
o-Xylene	0.20	0.10	0.30
m-Xylene	0.20	0.20	0.30
Ethylbenzene	0.40	0.40	0.30
C ₉ aromatics	0.10	1.10	0.90
C ₁₀ ⁺ aromatics	0.40	1.60	0.80

Data were taken at the eight hour of time-on-stream

Table 7.9 Composition of hydrocarbons obtained from using Cu-modified catalysts

Product	Sample		
	A ₂ O ₃	Cu/Al ₂ O ₃	Cu ₂ O/Al ₂ O ₃
Product Distribution (wt%)			
Oxygenates	92.1	87.2	88.9
Non-aromatics	0.60	0.40	0.20
Benzene	5.20	3.40	7.40
Toluene	0.60	1.10	0.90
p-Xylene	0.20	0.50	0.30
o-Xylene	0.20	0.40	0.20
m-Xylene	0.20	0.40	0.30
Ethylbenzene	0.40	0.30	0.20
C ₉ aromatics	0.10	2.10	0.80
C ₁₀ ⁺ -aromatics	0.40	4.30	0.70

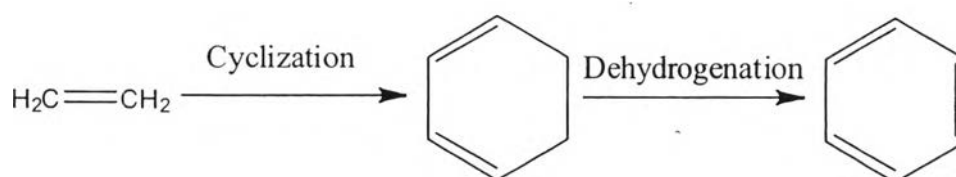
Data were taken at the eight hour of time-on-stream

Table 7.10 Composition of hydrocarbons obtained from using Pd-modified catalysts

Product	Sample		
	Al ₂ O ₃	Pd/Al ₂ O ₃	PdO/Al ₂ O ₃
Product Distribution (wt%)			
Oxygenates	92.1	39.4	75.5
Non-aromatics	0.60	0.40	0.10
Benzene	5.20	42.40	16.40
Toluene	0.60	1.30	1.00
p-Xylene	0.20	0.90	0.30
o-Xylene	0.20	1.30	0.30
m-Xylene	0.20	0.90	0.60
Ethylbenzene	0.40	0.50	0.40
C ₉ aromatics	0.10	0.50	1.10
C ₁₀ ⁺ - aromatics	0.40	12.40	4.30

Data were taken at the eight hour of time-on-stream

Therefore, the formation of hydrocarbons with using these catalysts can be explained as follows: Ethylene suppressed in the gaseous product is suspected to be an important intermediate to transform to various hydrocarbons in oil. Firstly, ethylene might undergo cyclization to form 1,3-cyclohexadiene as a primary hydrocarbon, and then undergo dehydrogenation, leading to benzene formation, as depicted in Figure 7.9. Moreover, benzene could undergo further reactions to form larger hydrocarbons. Additionally, using Ni, Cu, and Pd promoters in both metallic and metal oxide forms on Al₂O₃ support, the catalysts might promote similar pathway of ethylene chain growth as illustrated in Figure 7.9.

**Figure 7.9** Ethylene chain growth using Ni-, Cu-, and Pd-modified catalysts.

7.6.3 Oxygenate Compositions

From Figure 7.10 displays oxygenate compound compositions. It can be observed that the oxygenate compounds are composed of two main components; that are, phenol and ketone compounds. Moreover, the other group is a trace amount of ether compounds.

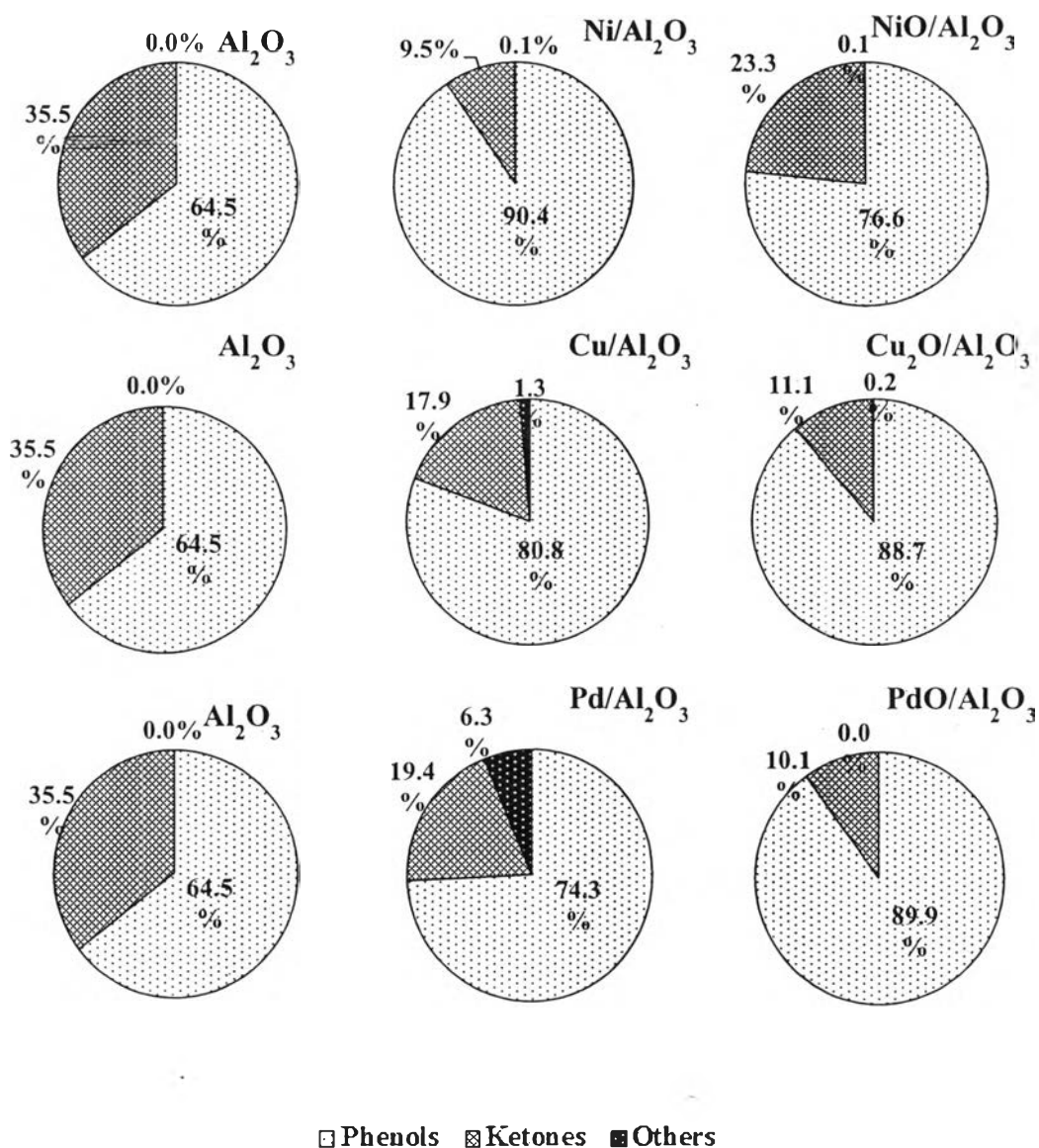


Figure 7.10 Compositions of oxygenate compounds (wt%) found in liquid products.

It is observed that all catalysts give similar components of oxygenate compounds. However, there is the difference in phenol compound selectivity when using Ni-modified Al_2O_3 catalysts in both metallic and metal oxide forms. As can be seen in Figure 7.10, using $\text{Ni}/\text{Al}_2\text{O}_3$ catalyst, phenol selectivity is significantly enhanced; however, using $\text{NiO}/\text{Al}_2\text{O}_3$ catalyst, it is slightly enhanced. For Cu- and Pd-modified Al_2O_3 catalysts, the catalysts significantly exhibit the increases in phenol selectivity; on the contrary, ketone selectivity is not significantly different from all catalysts. Moreover, it can be noticed that when using Ni-, Cu-, and Pd-modified Al_2O_3 catalysts, a trace amount of ether compound is observed. In addition, phenol selectivity, using metallic promoters, can be ranked in the order: $\text{Ni}/\text{Al}_2\text{O}_3 > \text{Cu}/\text{Al}_2\text{O}_3 > \text{Pd}/\text{Al}_2\text{O}_3 > \text{Al}_2\text{O}_3$; on the other hand, when using metal oxide promoters, the selectivity can be ranked as follows: $\text{PdO}/\text{Al}_2\text{O}_3 > \text{Cu}_2\text{O}/\text{Al}_2\text{O}_3 > \text{NiO}/\text{Al}_2\text{O}_3 > \text{Al}_2\text{O}_3$. Furthermore, ketone selectivity, using metallic promoters is decreased in the order: $\text{Al}_2\text{O}_3 > \text{Pd}/\text{Al}_2\text{O}_3 > \text{Cu}/\text{Al}_2\text{O}_3 > \text{Ni}/\text{Al}_2\text{O}_3$; however, the selectivity, when using metal oxide promoters, can be ranked in the order: $\text{Al}_2\text{O}_3 > \text{NiO}/\text{Al}_2\text{O}_3 > \text{Cu}_2\text{O}/\text{Al}_2\text{O}_3 > \text{PdO}/\text{Al}_2\text{O}_3$.

Moreover, phenol compounds are found as the major group of components in oxygenate compounds, and it is found as the major component using all Ni-modified catalysts as shown in Figure 7.11. It is significantly increased from 18.8 wt% to 38.4 wt% and 42.5 wt% by using $\text{Ni}/\text{Al}_2\text{O}_3$ and $\text{NiO}/\text{Al}_2\text{O}_3$ catalysts, respectively; in addition, phenol selectivity can be ranked in the order: $\text{NiO}/\text{Al}_2\text{O}_3 > \text{Ni}/\text{Al}_2\text{O}_3 > \text{Al}_2\text{O}_3$. Furthermore, the other major group of components in oxygenate compounds is ketone compounds. From Figure 7.12, among ketone compounds, 2-pentanone is slightly decreased from 81.4 wt% to 76.4 wt% and 67.7 wt% by using $\text{Ni}/\text{Al}_2\text{O}_3$ and $\text{NiO}/\text{Al}_2\text{O}_3$ catalysts, respectively. However, 3-pentanone is slightly increased from 3.7 wt% to 13.8 wt% and 8.1 wt%, by using $\text{Ni}/\text{Al}_2\text{O}_3$ and $\text{NiO}/\text{Al}_2\text{O}_3$, respectively. From the results, 2-pentanone selectivity can be ranked as a follows: $\text{Al}_2\text{O}_3 > \text{Ni}/\text{Al}_2\text{O}_3 > \text{NiO}/\text{Al}_2\text{O}_3$.

The compositions of oxygenate compounds in Figure 7.10 shows that the oxygenate compounds are composed of three main components; that are, phenol, ketone, and a trace of ether compounds. Compared to parent alumina, phenol compounds are increased from 64.5 wt% to 80.7 wt% and 88.7 wt% by using

Cu/Al₂O₃ and Cu₂O₃/Al₂O₃; however, ketone compounds are decreased from 35.5 wt% to 17.9 wt% and 11.1 wt% using Cu/Al₂O₃ and Cu₂O/Al₂O₃, respectively. As a result, it is observed that all catalysts give a high concentration of oxygenate compounds as obtained from unmodified Al₂O₃, indicating that all catalysts promote similar pathways of oxygenate compounds formation via ethanol dehydrogenation. Moreover, phenol is found as a major component in phenol compounds. From Figure 7.11, it is found that phenol selectivity is significantly increased from 18.8 wt% to 38.1 wt% and 49.6 wt% using Cu/Al₂O₃ and Cu₂O/Al₂O₃, respectively. So, the phenol selectivity is decreased in the following order: Cu₂O/Al₂O₃ > Cu/Al₂O₃ > Al₂O₃.

The compositions of ketone compounds in Figure 7.12 show that 2-pentanone is made dominantly from all catalysts; however, 2-pentanone selectivity is decreased from 84.1 wt% to 67.8 wt% and 62.5 wt% by using Cu/Al₂O₃ and Cu₂O/Al₂O₃, respectively. Therefore, 2-pentanone selectivity can be ranked in the order: Al₂O₃ > Cu/Al₂O₃ > Cu₂O/Al₂O₃.

The main components in oxygenate compounds using either Pd/Al₂O₃ and PdO/Al₂O₃ catalysts are shown in Figure 7.10. They are composed of phenol and ketone compounds. Compared to unmodified Al₂O₃, the selectivity of phenol compounds are slightly increased from 64.5 wt% to 74.3 wt% and 89.9 wt% using Pd/Al₂O₃ and PdO/Al₂O₃ catalysts, respectively. However, the selectivity of ketone compounds are slightly decreased from 35.5 wt% to 19.4 wt% and 89.9 wt% using Pd/Al₂O₃ and PdO/Al₂O₃ catalysts, respectively. As a result, the selectivity of phenol compounds can be ranked as follows: PdO/Al₂O₃ > Pd/Al₂O₃ > Al₂O₃, and the selectivity of ketone compounds can be ranked as follows: Al₂O₃ > Pd/Al₂O₃ > PdO/Al₂O₃. Moreover, the compositions of phenol compounds in Figure 7.11 shows that phenol is found as a main component in phenol compounds obtained from using both Pd/Al₂O₃ and PdO/Al₂O₃ catalysts. Compared to pure Al₂O₃, phenol selectivity is significantly increased from 18.8 wt% to 67.9 wt% 47.0 wt% using Pd/Al₂O₃ and PdO/Al₂O₃ catalysts, respectively. So, the phenol selectivity can be ranked in the order: Pd/Al₂O₃ > PdO/Al₂O₃ > Al₂O₃. Furthermore, the compositions of ketone compounds obtained from all catalysts are displayed in Figure 7.12. It is observed that 2-pentanone is made dominantly from all catalysts. However, the introduction of

metallic Pd and PdO on alumina surface, 2-pentanone is slightly decreased in the order: PdO/Al₂O₃ > Pd/Al₂O₃ > Al₂O₃.

The compositions of phenol products in Figure 7.11 show that phenol is found as the major component with using Ni-, Cu-, and Pd-modified Al₂O₃ catalysts. Moreover, when using metallic promoters, phenol selectivity can be ranked in the order: Pd/Al₂O₃ > Ni/Al₂O₃ > Cu/Al₂O₃ > Al₂O₃; on the other hand, using metal oxide promoters, phenol selectivity can be ranked as follows: Cu₂O/Al₂O₃ > PdO/Al₂O₃ > NiO/Al₂O₃ > Al₂O₃. In addition, the other major group of components in oxygenate compounds is ketone products. From Figure 7.12, among ketone products, 2-pentanone is found as the major component in ketone products. When using metal promoters, 2-pentanone selectivity are decreased as follows: Al₂O₃ = Pd/Al₂O₃ > Ni/Al₂O₃ > Cu/Al₂O₃; however, using metal oxide promoters, 2-pentanone selectivity are decreased as follows: Al₂O₃ > PdO/Al₂O₃ > NiO/Al₂O₃ > Cu₂O/Al₂O₃.

As a result, when the composition of oxygenate compounds obtained from all catalysts, it can be concluded that both metallic and metal oxide promoters promote similar pathways of oxygenate compounds formation through ethanol dehydrogenation. Generally, dehydrogenation reaction is widely catalyzed by using metal oxide catalysts due to the formation of oxygen vacancies on metal oxide surface. Another reason is Al₂O₃ support that is classified as a type of metal oxide; hence, the formation of oxygenate compounds is governed by Al₂O₃ support as well. Additionally, when the oxygen vacancies are formed, hydrogen atom of hydrocarbons or organic compounds can be abstracted by these vacancies, leading to dehydrogenation reaction.

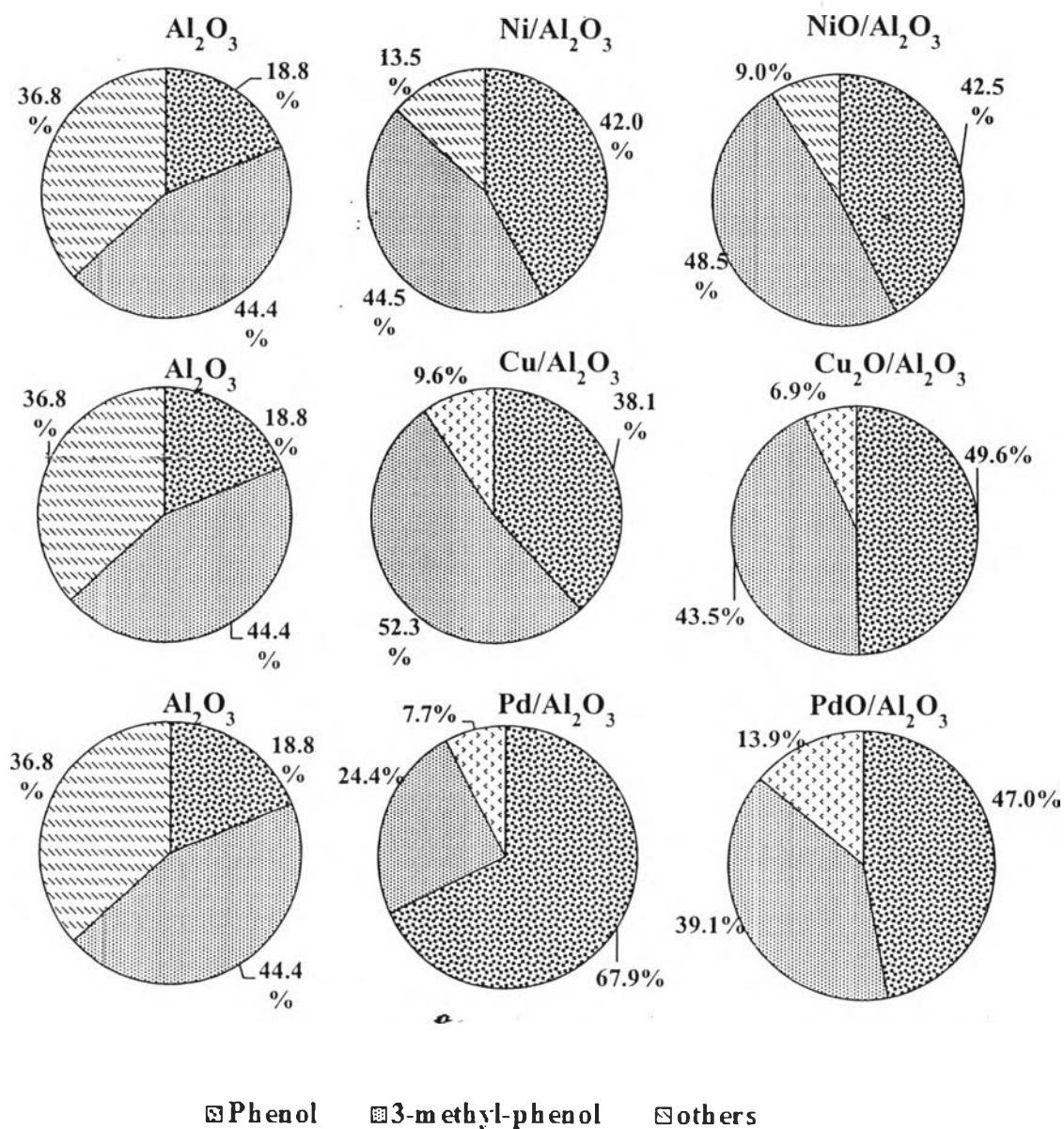


Figure 7.11 Compositions of phenols (wt%) found in oxygenate compounds using Ni-, Cu-, and Pd-modified catalysts.

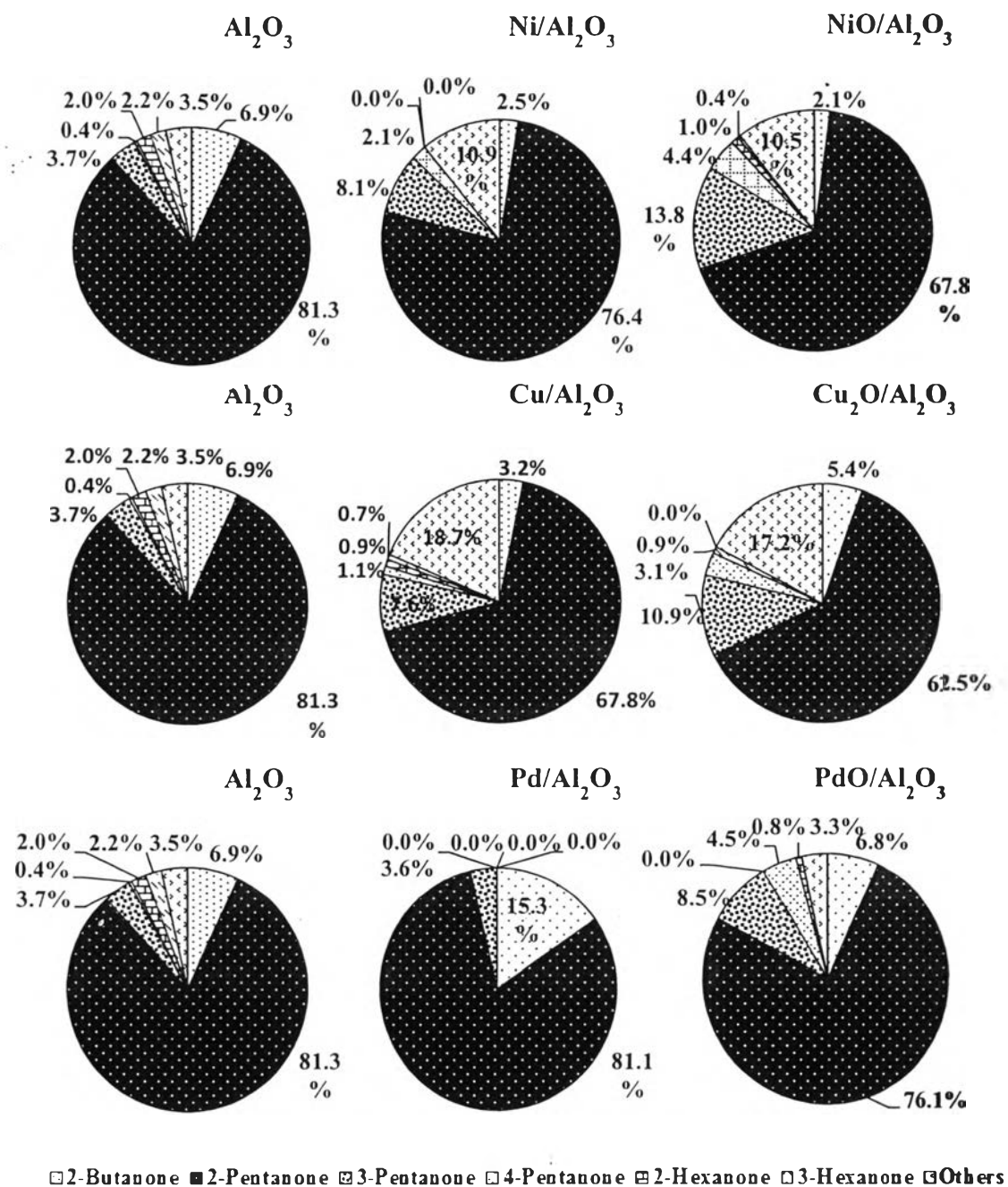


Figure 7.12 Compositions of ketones (wt%) found in oxygenate compounds using Ni-, Cu-, and Pd-modified catalysts.

7.7 Effect of Oxidation States

Two different oxidation states of Ni-, Cu-, and Pd-modified catalysts are examined, aiming to investigate the effect of oxidation state on product distribution in the catalytic dehydration of bio-ethanol. Therefore, oxygenate and hydrocarbon yields play an important role on determination the reaction pathways and product distributions. As seen in Table 7.7, the oxygenate compounds are slightly decreased; however, the hydrocarbons are slightly increased by using nickel-modified catalysts as compared to Al_2O_3 . This implies that both metallic Ni and NiO-modified catalysts promote similar outstanding reaction; that is, ethanol dehydration rather than ethanol dehydrogenation. From the results, the modified catalysts promote similar reaction pathways of ethylene chain growth, but exhibit different ability. The catalytic activity for producing hydrocarbons can be ranked in the order: $\text{Ni}/\text{Al}_2\text{O}_3 > \text{NiO}/\text{Al}_2\text{O}_3$. Generally, metallic Ni is generally used in hydrogenation of hydrocarbons, and widely used to produce various kinds of hydrocarbons, for example, ethylene oligomerization (Lallemand *et al.*, 2006), and ethylene polymerization (Miyakoshi *et al.*, 2006). Moreover, the catalysts displayed high activity to produce hydrocarbons; thus, in the catalytic dehydration of bio-ethanol, metallic nickel-promoted catalyst might promote higher activity than that $\text{NiO}/\text{Al}_2\text{O}_3$. In addition, $\text{NiO}/\text{Al}_2\text{O}_3$ catalyst is widely employed in dehydrogenation because the catalyst has oxygen vacancies in the surface, which allows hydrogen to be abstracted from hydrocarbons, leading to dehydrogenation. Therefore, NiO-modified catalyst promotes higher oxygenate compounds than metallic Ni-modified catalysts, and the ability to produce oxygenate compounds can be ranked in the order of $\text{NiO}/\text{Al}_2\text{O}_3 > \text{Ni}/\text{Al}_2\text{O}_3$.

Metallic $\text{Cu}/\text{Al}_2\text{O}_3$ and $\text{Cu}_2\text{O}/\text{Al}_2\text{O}_3$ catalysts were examined for the effect of oxidation states on product distributions in the catalytic dehydration of bio-ethanol. From the result, it can be noticed that using $\text{Cu}/\text{Al}_2\text{O}_3$ and $\text{Cu}_2\text{O}/\text{Al}_2\text{O}_3$ catalysts, the hydrocarbons yield are slightly enhanced, while oxygenates yield are slightly suppressed, indicating that both $\text{Cu}/\text{Al}_2\text{O}_3$ and $\text{Cu}_2\text{O}/\text{Al}_2\text{O}_3$ catalysts have less ability to produce hydrocarbons. Therefore, ethanol dehydration might be promoted as dominant reaction in the catalytic dehydration of bio-ethanol. Moreover, the ability to produce hydrocarbons can be ranked in the order of $\text{Cu}/\text{Al}_2\text{O}_3 >$

$\text{Cu}_2\text{O}/\text{Al}_2\text{O}_3$. Moreover, the insignificant difference in the suppression of oxygenate compounds may be explained by the ease of oxidation of copper when exposed to air or oxidizing agent. Moreover, it is found that copper and oxygen have the electronegativity numbers (E_n) equal to 1.90 and 3.44, respectively. This means that copper is able to donate an outermost valence electron to oxygen easily, resulting in the transformation of metallic Cu to copper oxide. Generally, metal oxide catalysts are mostly used to stimulate dehydrogenation reaction due to the formation of oxygen vacancies on their surface. Metallic Cu has been used in methanol partial oxidation to produce aldehyde. Bluhm *et al.*, (2004) found that metallic Cu was an un-active site for producing aldehyde until it was transformed to copper oxide because there was the formation of subsurface oxygen on copper catalyst that led to the abstraction of hydrogen.

For Pd-modified catalysts, it can be noticed that both metallic and palladium oxide promoters promote similar pathways of ethanol transformation; that is, ethanol dehydration, due to the significant increase in hydrocarbon products in oils. However, they have different ability to produce hydrocarbons. As seen Table 7.5, the hydrocarbons are considerably increased to 24.5 wt% and 60.4 wt% when oxidation state of palladium is changed from 2+ to 0, meaning that metallic Pd/ Al_2O_3 catalyst has higher ability than PdO/ Al_2O_3 catalyst. Jung *et al.*, (2015) reported that palladium-promoted catalysts have high ability to accelerate the formation of carbon-carbon bond, and have high hydrogen adsorption capacity to absorb hydrogen at room temperature forming palladium hydride (PdH_x) (Hao *et al.*, 2015). Therefore, palladium is widely employed in cross-couplings, hydrogenation and hydrogenolysis reaction. Moreover, the change of oxidation states also affects to oxygenate compounds; which are considerably decreased to 75.5 wt% and 39.6 wt% by using PdO/ Al_2O_3 and Pd/ Al_2O_3 catalysts, respectively. It is evident that PdO is partially reduced to Pd after the catalytic testing, confirmed by the result of XPS analysis. This can be explained that the reduction of oxygen adatom on PdO surface leads to the reduction of anion vacancies, resulting in the decrease in oxygenate compounds because ethanol dehydrogenation reaction is not promoted outstandingly.

Additionally, the ability to produce hydrocarbons can be ranked as follows: Pd/Al₂O₃ > PdO/Al₂O₃ > Al₂O₃.

In conclusion, using metallic promoters, the ability to produce hydrocarbons can be ranked as follows: Pd/Al₂O₃ > Ni/Al₂O₃ > Cu/Al₂O₃ > Al₂O₃; however, using metal oxide promoters, the ability is decreased in the order: Al₂O₃ > Cu₂O/Al₂O₃ > NiO/Al₂O₃ > PdO/Al₂O₃.

7.8 Pathways of Ethanol Transformation

The pathways of ethanol transformation using Ni-, Cu-, and Pd-modified Al₂O₃ catalysts are depicted in Figure 7.13. When bio-ethanol is fed and passed through the catalysts, the formation of oxygenate ethylene and oxygenate compounds are governed by Al₂O₃ support. Moreover, the formation of oxygenate compounds on Al₂O₃ support relates to the formation of anion vacancies because Al₂O₃ is classified as a kind of metal oxide that contains oxygen vacancies. In general, dehydrogenation reaction can be occurred with using metal oxide catalysts. Therefore, ethanol dehydrogenation can be promoted when Al₂O₃ catalyst is employed. Furthermore, the formation of ethylene is also governed by Al₂O₃ support due to acid property of alumina that can drive ethanol dehydration. In addition, with the addition of Ni, Cu, and Pd in both metallic and metal oxide forms on Al₂O₃ surface, the oxygenate compounds are suppressed whereas the hydrocarbons are enhanced, meaning that Ni, Cu, and Pd in both forms govern the formation of hydrocarbon production, but they have different ability by promoting hydrocarbon formation through cyclization and dehydrogenation reaction. Additionally, different oxidation states of Ni, Cu, and Pd do not affect to product distribution. When metallic and metal oxide promoters are compared, it is found that the metallic promoter gives higher hydrocarbon production than the metal oxide promoter. Furthermore, the formation of a non-aromatic compound; that is 1,3-cyclohexadiene, is observed before being transformed to benzene.

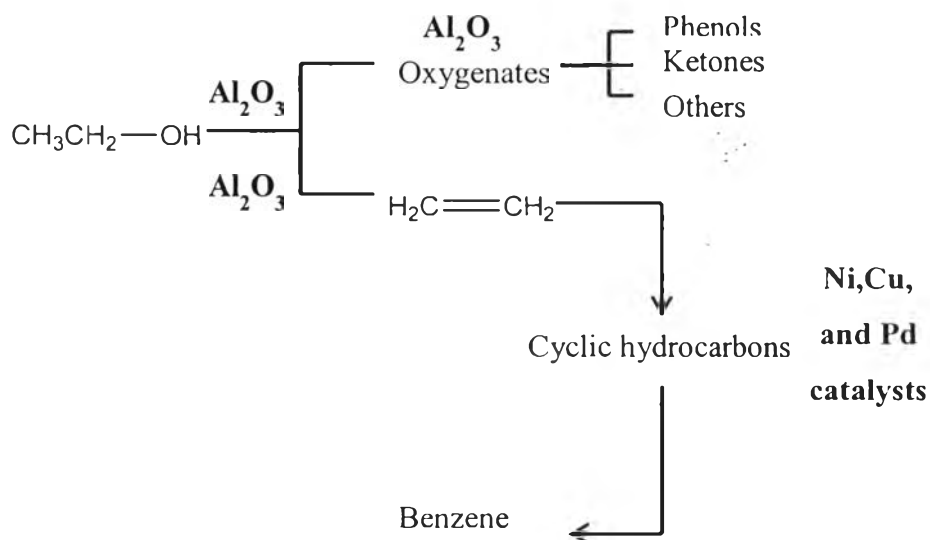


Figure 7.13 Ethanol transformation pathways using Ni-, Cu-, and Pd-modified catalysts.

7.9 Conclusions

In conclusion, different oxidation states of metal catalysts such as Ni, Cu and Pd were examined in the catalytic dehydration of bio-ethanol, aiming to investigate the effect of oxidation state on the product distribution. From the results, it can be concluded that the used of Ni, Cu, and Pd as a promoter on alumina support resulted in the suppression of oxygenate compounds whereas the hydrocarbons were enhanced. When metal and metal oxide catalysts were compared, it was found that metal catalysts had higher ability to produce hydrocarbon than metal oxide catalysts. Moreover, the ability to produce hydrocarbons can be ranked in the order of: $\text{Pd}/\text{Al}_2\text{O}_3 > \text{Ni}/\text{Al}_2\text{O}_3 > \text{Cu}/\text{Al}_2\text{O}_3 > \text{Al}_2\text{O}_3$. Moreover, most of the obtained hydrocarbons were aromatics; however, there was a formation of cyclic compound; that is, 1,3-cyclohexadiene, which is believed to be an important intermediate to be further transformed to various aromatics in the liquid product. In addition, all catalysts promoted the similar pathways of ethylene chain growth. Additionally, when noble (Pd) and non-noble (Ni and Cu) promoters in different oxidation states

were compared, it was found that in the case of metal promoter, 1wt% Pd/Al₂O₃ exhibited the highest ability to produce hydrocarbons; and 1 wt% PdO/Al₂O₃ exhibited the highest ability to produce hydrocarbons among the metal oxide promoters.

7.10 References

- Akgul, F.A., Akgul, G., Yildirim, N., Unalan, H.E., and Turan, R. (2014) Influence of thermal annealing on microstructural, morphological, optical properties and surface electronic structure of copper oxide thin films. Materials Chemistry and Physics, 147(3), 987-995.
- Barthélémy, B., Devillers, S., Minet, I., Delhalle, J., and Mekhalif, Z. (2011) Induction heating for surface triggering styrene polymerization on titanium modified with ATRP initiator. Journal of Colloid and Interface Science, 354(2), 873-879.
- Biesinger, M.C., Lau, L.W.M., Gerson, A.R., and Smart, R.S.C. (2010) Resolving surface chemical states in XPS analysis of first row transition metals, oxides and hydroxides: Sc, Ti, V, Cu and Zn. Applied Surface Science, 257(3), 887-898.
- Biesinger, M.C., Payne, B.P., Grosvenor, A.P., Lau, L.W.M., Gerson, A.R., and Smart, R.S.C. (2011) Resolving surface chemical states in XPS analysis of first row transition metals, oxides and hydroxides: Cr, Mn, Fe, Co and Ni. Applied Surface Science, 257(7), 2717-2730.
- Bluhm, H., Hävecker, M., Knop-Gericke, A., Kleimenov, E., Schlögl, R., Teschner, D., Bukhtiyarov, V.I., Ogletree, D.F., and Salmeron, M. (2004) Methanol Oxidation on a Copper Catalyst Investigated Using in Situ X-ray Photoelectron Spectroscopy. The Journal of Physical Chemistry B, 108(38), 14340-14347.
- Brun, M., Berthet, A., and Bertolini, J.C. (1999) XPS, AES and Auger parameter of Pd and PdO. Journal of Electron Spectroscopy and Related Phenomena, 104(1-3), 55-60.
- Cai, T. (1999). Studies of a new alkene oligomerization catalyst derived from nickel

- sulfate. Catalysis Today, 51(1), 153-160.
- Cheng, Z., Zhu, X., Zhou, N., Zhu, J., and Zhang, Z. (2005) Atom transfer radical polymerization of styrene under pulsed microwave irradiation. Radiation Physics and Chemistry, 72(6), 695-701.
- Guan, Y., Li, Y., van Santen, R., Hensen, E.M., and Li, C. (2007) Controlling Reaction Pathways for Alcohol Dehydration and Dehydrogenation over FeSBA-15 Catalysts. Catalysis Letters, 117(1-2), 18-24.
- Guo, L., Zhou, J., Mao, J., Guo, X., and Zhang, S. (2009) Supported Cu catalysts for the selective hydrogenolysis of glycerol to propanediols. Applied Catalysis A: General, 367(1-2), 93-98.
- Hao, Y., Wang, X., Perret, N., Cárdenas-Lizana, F., and A.Keane, M. (2015) Support effects in the gas phase hydrogenation of butyronitrile over palladium. Catalysis, Structure & Reactivity, 1(1), 4-10.
- Hodgkinson, J.L., Massey, D., and Sheel, D.W. (2013) The deposition of copper-based thin films via atmospheric pressure plasma-enhanced CVD. Surface and Coatings Technology, 230(0), 260-265.
- Huang, S., Zhang, C., and He, H. (2013) Effect of pretreatment on Pd/Al₂O₃ catalyst for catalytic oxidation of o-xylene at low temperature. Journal of Environmental Sciences, 25(6), 1206-1212.
- Hulea, V. and Fajula, F. (2004) Ni-exchanged AlMCM-41—An efficient bifunctional catalyst for ethylene oligomerization. Journal of Catalysis, 225 (1), 213-222.
- Jung, U., Elsen, A., Li, Y., Smith, J.G., Small, M.W., Stach, E.A., Frenkel, A.I., and Nuzzo, R.G. (2015) Comparative in Operando Studies in Heterogeneous Catalysis: Atomic and Electronic Structural Features in the Hydrogenation of Ethylene over Supported Pd and Pt Catalysts. ACS Catalysis, 5(3), 1539-1551.
- Lallemand, M., Finiels, A., Fajula, F., and Hulea, V. (2006) Catalytic oligomerization of ethylene over Ni-containing dealuminated Y zeolites. Applied Catalysis A: General, 301(2), 196-201.
- Li, G., Hu, L., and Hill, J.M. (2006) Comparison of reducibility and stability of alumina-supported Ni catalysts prepared by impregnation and co-

- precipitation. Applied Catalysis A: General, 301(1), 16-24.
- Li, K., Darkwa, J., Guzei, I.A., and Mapolie, S.F. (2002) Synthesis and evaluation of substituted pyrazoles palladium(II) complexes as ethylene polymerization catalysts. Journal of Organometallic Chemistry, 660(1), 108-115.
- Liu, C., Li, J., Zhang, Y., Chen, S., Zhu, J., and Liew, K. (2012) Fischer–Tropsch synthesis over cobalt catalysts supported on nanostructured alumina with various morphologies. Journal of Molecular Catalysis A: Chemical, 363–364(0), 335-342.
- Martínez, A., Arribas, M.A., Concepción, P. and Moussa, S. (2013) New bifunctional Ni–H-Beta catalysts for the heterogeneous oligomerization of ethylene. Applied Catalysis A: General 467, 509-518.
- Miyakoshi, R., Yokoyama, A., and Yokozawa, T. (2005) Catalyst-Transfer Polycondensation. Mechanism of Ni-Catalyzed Chain-growth Polymerization Leading to Well-Defined Poly(3-hexylthiophene). Journal of the American Chemical Society, 127(49), 17542-17547.
- Mkoyi, H.D., Ojwach, S.O., Guzei, I.A., and Darkwa, J. (2013) (Pyrazol-1-yl) carbonyl palladium complexes as catalysts for ethylene polymerization reaction. Journal of Organometallic Chemistry, 724, 95-101.
- Musolino, M.G., Caia, C.V., Mauriello, F., and Pietropaolo, R. (2010) Hydrogenation versus isomerization in the reaction of cis-2-butene-1,4-diol over supported catalysts: The role of Group VIII transition metals in driving the products selectivity. Applied Catalysis A: General, 390(1–2), 141-147.
- Salagre, P., Fierro, J.L.G., Medina, F., and Sueiras, J.E. (1996) Characterization of nickel species on several γ -alumina supported nickel samples. Journal of Molecular Catalysis A: Chemical, 106(1–2), 125-134.